Disease Models & Mechanisms 5, 63-72 (2012) doi:10.1242/dmm.008367

An inducible *kras^{V12}* transgenic zebrafish model for liver tumorigenesis and chemical drug screening

Anh Tuan Nguyen[1,2], Alexander Emelyanov[2,*], Chor Hui Vivien Koh[1,*], Jan M. Spitsbergen[3], Serguei Parinov[2,‡] and Zhiyuan Gong[1,‡]

SUMMARY

Because Ras signaling is frequently activated by major hepatocellular carcinoma etiological factors, a transgenic zebrafish constitutively expressing the *kras^{V12}* oncogene in the liver was previously generated by our laboratory. Although this model depicted and uncovered the conservation between zebrafish and human liver tumorigenesis, the low tumor incidence and early mortality limit its use for further studies of tumor progression and inhibition. Here, we employed a mifepristone-inducible transgenic system to achieve inducible *kras^{V12}* expression in the liver. The system consisted of two transgenic lines: the liver-driver line had a liver-specific *fabp10* promoter to produce the LexPR chimeric transactivator, and the Ras-effector line contained a *LexA*-binding site to control *EGFP-kras^{V12}* expression. In double-transgenic zebrafish (driver-effector) embryos and adults, we demonstrated mifepristone-inducible *EGFP-kras^{V12}* expression in the liver. Robust and homogeneous liver tumors developed in 100% of double-transgenic fish after 1 month of induction and the tumors progressed from hyperplasia by 1 week post-treatment (wpt) to carcinoma by 4 wpt. Strikingly, liver tumorigenesis was found to be 'addicted' to Ras signaling for tumor maintenance, because mifepristone withdrawal led to tumor regression via cell death in transgenic fish. We further demonstrated the potential use of the transparent *EGFP-kras^{V12}* larvae in inhibitor treatments to suppress Ras-driven liver tumorigenesis by targeting its downstream effectors, including the Raf-MEK-ERK and PI3K-AKT-mTOR pathways. Collectively, this mifepristone-inducible and reversible *kras^{V12}* transgenic system offers a novel model for understanding hepatocarcinogenesis and a high-throughput screening platform for anti-cancer drugs.

INTRODUCTION

Hepatocellular carcinoma (HCC) is the most common and malignant type of liver cancer and causes approximately 0.6 million deaths each year (Gomaa et al., 2008). The incidence and mortality rates of HCC have increased worldwide, and most patients are diagnosed at late stages, when therapies are less effective (Farazi and DePinho, 2006). Thus, an improved understanding of its molecular pathogenesis is desirable for development of new systemic therapies. Recently, high-throughput genomic technologies have enabled large numbers of samples to be analyzed and have uncovered important oncogenes and signaling pathways that are associated with HCC progression (Zender et al., 2006; Villanueva and Llovet, 2011). Being a potent proto-oncogene and bona fide central regulator of several signal transduction pathways in many human cancers, Ras is at the leading edge of most tumorigenic events and is activated in as many as 50% of all HCC cases (Downward, 2003; Villanueva and Llovet, 2011). Importantly, activation of the Raf-MEK-ERK and PI3K-AKT-mTOR pathways, which are major downstream effectors of Ras, has been reported in human HCCs (Downward, 2003; Schmidt et al., 1997; Calvisi et al., 2006; Newell et al., 2009). Indeed, pharmacological inhibition of these pathways has exhibited significant anti-tumoral effects in clinical trials (Llovet and Bruix, 2008).

The zebrafish is a powerful vertebrate model in cancer research owing to its feasibility for high-throughput forward genetics and chemical screens (Amatruda and Patton, 2008; Zon and Peterson, 2005). In recent years, a number of transgenic zebrafish lines have been developed and, in general, these faithfully mimicked human diseases, including leukemia, melanoma, embryonal rhabdomyosarcoma and others (Lam et al., 2006; Langenau et al., 2003; Langenau et al., 2007; Liu and Leach, 2011; Patton et al., 2005). Recently, we reported the first transgenic zebrafish liver cancer model by constitutively overexpressing oncogenic *kras^{V12}* under a hepatocyte-specific promoter (Nguyen et al., 2011). Although this model has revealed several molecular mechanisms underlying Ras-driven liver tumorigenesis and recapitulated the typical hallmarks of human HCC, a constitutively high level of Ras expression caused early tumorigenesis and mortality. In a low-*kras^{V12}*-expression strain, tumor onset is relatively late and tumor occurrence is comparatively low (approximately 30%), consequently hindering the use of this model for large-scale studies and drug screens.

To address these limitations, we employed the mifepristone-inducible LexPR system (Emelyanov and Parinov, 2008) in this study to conditionally control the liver-specific expression of *EGFP-kras^{V12}* in transgenic fish. Here, we demonstrated that this strategy allowed temporally controlled *kras^{V12}* expression in both embryonic and adult transgenics in a dosage-dependent manner. Rapid *kras^{V12}*

[1]Department of Biological Sciences, National University of Singapore, Singapore, 117543
[2]Temasek Life Sciences Laboratory, National University of Singapore, Singapore, 117604
[3]Department of Microbiology and Marine and Freshwater Biomedical Sciences Center, Oregon State University, Corvallis, OR 97331, USA
*These authors contributed equally to this work
‡Authors for correspondence (sergeypa@tll.org.sg; dbsgzy@nus.edu.sg)

Received 20 June 2011; Accepted 8 August 2011

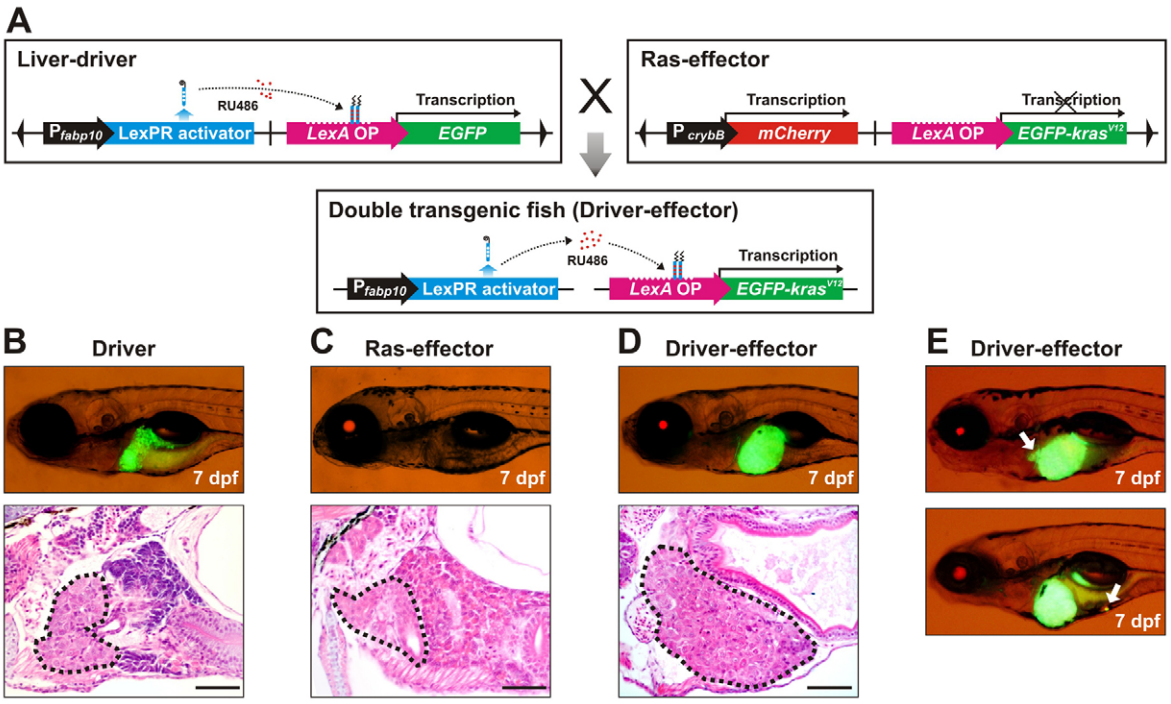

Fig. 1. Mifepristone-inducible liver-specific *kras*^{V12} expression in transgenic zebrafish. (A) Schematic diagram of the mifepristone-inducible LexPR system with separate liver-driver and Ras-effector constructs. The liver-specific expression of *EGFP-kras*^{V12} in double-transgenic fish (driver-effector), harboring both cassettes, is activated in trans by the LexPR activator produced from the liver-driver in the presence of mifepristone (RU486). (B-E) Representative 7-dpf fry from the liver-driver (B), Ras-effector (C) and driver-effector double transgenics (D,E). All fry were incubated with 1 μM mifepristone from 3 dpf. The upper panels show a fluorescent image and the lower panels show histology. The liver-driver fry had induced EGFP expression in the liver and a normal liver histology (B). The Ras-effector fry had mCherry expression in the lens as a transgenic marker but no induced EGFP expression in the liver, and also had a normal liver histology (C). *EGFP-kras*^{V12} expression was induced in driver-effector double-transgenic larvae at 3 dpf, causing the development of an enlarged and hyperplastic liver (D) and some individuals showed invasive EGFP-positive cells as indicated by arrows (E). Dotted areas indicate the liver regions. Scale bars: 50 μm.

tumor progression was observed in this inducible model after mifepristone administration. Strikingly, removal of mifepristone led to rapid tumor regression, supporting the concept of 'oncogene addiction' for tumor maintenance. Furthermore, treatments with chemical inhibitors of the Raf-MEK-ERK and/or PI3K-AKT-mTOR pathways resulted in effective suppression of hyperplastic growth of the liver in *kras*^{V12} transgenic fry. Thus, the high tumor incidence (100%) and convenience of chemical treatment in this inducible model might allow it to be used for detailed analyses of liver tumor progression and/or regression as well as for potential anti-cancer drug screens.

RESULTS

Generation of mifepristone-inducible *kras*^{V12} transgenic zebrafish

Using the mifepristone-inducible LexPR system (Emelyanov and Parinov, 2008), two stable transgenic zebrafish lines (driver and effector) were generated. As depicted in Fig. 1A, the liver-driver line, *Tg(fabp10:LexPR; LexA:EGFP)*, expressed the LexPR transactivator in the liver under control of the liver-specific *fabp10* promoter (previously named *lfabp*) (Her et al., 2003; Korzh et al., 2008); LexPR then bound to the *LexA* operator in the presence of mifepristone and induced the synthesis of EGFP as a reporter for transgenic identification, as confirmed in Fig. 1B. The Ras-effector line, *Tg(cryB:mCherry; LexA:EGFP-kras*^{V12}*)*, contained a selection marker, *mCherry*, driven by the zebrafish *crybB* (*crystallin beta B*) promoter, which produced red fluorescence in the lens (Fig. 1C). In the Ras-effector line, the expression of the *EGFP-kras*^{V12} fusion gene was controlled by the *LexA* operator through binding to the LexPR transactivator. Crossing the liver-driver and Ras-effector lines resulted in double-transgenic offspring, which were capable of expressing *EGFP-kras*^{V12} exclusively in the liver upon administration of mifepristone (Fig. 1D).

To examine the effects of *kras*^{V12} expression, F_2 driver-effector double-transgenic fish were treated with 1 μM mifepristone from 3 days post-fertilization (dpf) onwards. At 7 dpf, the liver was greatly enlarged with 100% penetrance (Fig. 1D). In some individuals (<5%), some GFP-positive liver cells eventually shed out from the liver and even migrated along the abdominal cavity, indicating signs of metastasis (Fig. 1E). Histological analysis revealed that early activation of *kras*^{V12} caused hyperplastic liver (HL) and early HCC in transgenic larvae (Fig. 1D), as compared with the normal livers in the liver-driver alone (Fig. 1B) and Ras-effector alone (Fig. 1C) controls. Moreover, induced larvae started to die from 10 dpf, thus confirming the toxicity and oncogenicity of *kras*^{V12} during embryonic development.

Liver tumor progression and regression in *kras*^{V12} transgenic zebrafish

To avoid oncogenic toxicity during the embryonic stage, *kras*^{V12} expression was induced in the driver-effector double-transgenic fish

at 1 month of age. Mifepristone (RU486) concentration was first tested at 0.1, 0.5, 1, 2 and 5 μM (n=8 in each group) for 3 days. Liver mRNAs were isolated from different treatment groups and reverse transcriptase (RT)-PCR was performed to monitor the levels of $kras^{V12}$ transcripts. As shown in Fig. 2A, $kras^{V12}$ transcripts were induced by all tested mifepristone concentrations. Notably, increasing concentrations of mifepristone led to increasing $kras^{V12}$ transcripts, with the highest level obtained at 2-5 μM. By contrast, no $kras^{V12}$ transcript was detected in the driver-effector double-transgenic fish in the absence of mifepristone, indicating the tight control of the inducible system without leaky expression. To demonstrate the feasibility of switching off $kras^{V12}$ expression by mifepristone removal, driver-effector transgenic fish induced with 2 μM mifepristone for 3 days were transferred to mifepristone-free water. RT-PCR analysis indicated no detectable $kras^{V12}$ transcripts in these fish after 7 days of mifepristone withdrawal (Fig. 2A). These observations indicated that $kras^{V12}$ expression could be reversibly switched on and off by the addition and removal of mifepristone, respectively.

To induce liver tumors in the driver-effector double-transgenic fish, fish were treated with mifepristone in several concentration groups starting from 1 month of age for at least 6 months (n=20 in each group) and the rates of liver tumor occurrence were determined. Again, there was a dosage-dependent induction of liver tumors (Fig. 2B). Whereas fish treated with the low dosage had a lower frequency of liver tumors and longer treatment period before tumors appeared, both the 2 and 5 μM groups showed full tumor penetrance (100%) after 1 month of mifepristone induction. Because there was no significant difference in tumor penetrance and latent time between the 2 and 5 μM mifepristone treatments, 2 μM mifepristone was chosen in subsequent experiments.

Next, detailed study of $kras^{V12}$-induced tumor progression was conducted on 100 driver-effector fish maintained in water containing 2 μM mifepristone. Gross morphological and histological analyses were performed weekly on 15 randomly selected driver-effector fish to monitor tumor development. These analyses showed robust tumorigenesis starting from HL to full-blown HCC within 4 weeks of induction (Fig. 2C). During tumor progression, increasing liver tumor volume was observable by strong EGFP fluorescence. Strikingly, 100% of induced driver-effector fish developed HL after 1 week and then progressed to homogeneous HCC after 4 weeks (Fig. 2D). Notably, no adenoma was observed in induced transgenics.

To investigate whether tumor maintenance requires continual $kras^{V12}$ expression, a group of 15 double-transgenic fish with apparent liver tumors was transferred to mifepristone-free water. Interestingly, mifepristone-induced liver tumors regressed, with gradual loss of EGFP fluorescence (Fig. 2E). Histological examination revealed tumor shrinkage showing extensive scarring at the peripheral or focal tumor region in 100% of double-transgenic fish after mifepristone withdrawal. Notably, complete tumor regression with scarred fibrosis of the former tumor tissue was observed after 4 weeks of mifepristone withdrawal. By contrast, continual treatment (no mifepristone removal) of the double-transgenic fish for 8 weeks or longer resulted in extensive growth of malignant hepatoblastoma in HCC with mixed components of low- to high-grade carcinoma (mixed HCC) (Fig. 2D), and even in the development of ascites or invasive HCC (supplementary material Fig. S1). At this stage, the time required for tumor regression was lengthened and 5-10% of induced transgenics showed non-regressed tumors (data not shown). By comparison, the non-induced double-transgenic fish retained normal hepatic tissue (Fig. 3D, top panel).

Requirement of both the ERK and AKT pathways for $kras^{V12}$-driven liver tumorigenesis and tumor maintenance

To assess whether the Raf-MEK-ERK pathway is required during liver tumor progression and regression in the current model, western blot analysis was carried out using liver lysates from four groups: control (non-induced double-transgenic fish with normal liver), HL (induced for 2 weeks), HCC (induced for 4 weeks) and regressed (induced for 4 weeks followed by 2 weeks of mifepristone withdrawal) (Fig. 3A). Immunoblotting with anti-Kras (F234) for total Kras protein and anti-Kras-2B (C19) for $Kras^{V12}$ mutant protein showed that high levels of $Kras^{V12}$ protein were observed only in the HL and HCC groups, as compared with control. Owing to strong induction, a slightly higher level of $Kras^{V12}$ was detected in the regressed samples than that in the control. The level of phosphorylated ERK1/2 protein was elevated in the HL and HCC groups but decreased during tumor regression.

Apart from the ERK pathway, the phosphatidylinositol-3 kinase (PI3K) pathway is another well-characterized effector of Ras. Activation of PI3K-AKT leads to increased phosphorylation of AKT, which activates mTOR and this, in turn, phosphorylates the ribosomal protein S6 in human cancers (Downward, 2003). Immunoblotting using anti-phospho-AKT and anti-phospho-S6 showed elevated levels of these proteins in $kras^{V12}$ HL and HCC groups, whereas their expressions were decreased during tumor regression. Immunohistochemistry further confirmed that the hyperactivation of these two pathways is associated with $kras^{V12}$ liver tumor progression (Fig. 3B). In the regressed HCC fish, although reduced phospho-ERK1/2 and phospho-AKT stainings were observed in the remaining tumor mass, these signals were completely void in the scar. TUNEL staining indicated that the tumor scar contained abundant apoptotic cells; thus, suppression of Ras signaling caused tumor shrinkage primarily owing to apoptosis (Fig. 3B).

Prevention of $kras^{V12}$ liver tumorigenesis by inhibition of the ERK and/or AKT pathways

To further investigate the molecular mechanisms of $kras^{V12}$-induced hepatocarcinogenesis and to demonstrate the potential of the transgenic model for anti-cancer drug screening, several inhibitors targeting the ERK and/or AKT pathways were selected to validate the involvement of these key signaling pathways. Generally, the mifepristone-induced double-transgenic larvae were co-treated with mifepristone and inhibitor(s) at 3-3.5 dpf, and liver morphology was then examined at 7 dpf under a fluorescent microscope. To evaluate inhibitor efficacy, liver size of treated larvae was classified into three categories: 'normal' (liver size comparable to normal liver in driver transgenics), 'huge' (the liver was apparently hyperplastic) and 'large' (larger than normal liver but smaller than 'huge') (Fig. 1B,D). As shown in Fig. 4A,B, treatment with MEK1/2 inhibitor PD98059 at 10 μM resulted in the inhibition of hyperplastic liver growth in 49% of $kras^{V12}$ transgenic larvae. Similarly, inhibition of PI3K-AKT-mTOR signaling by targeting either PI3K with 10 μM LY294002 or mTOR with 0.7 μM rapamycin

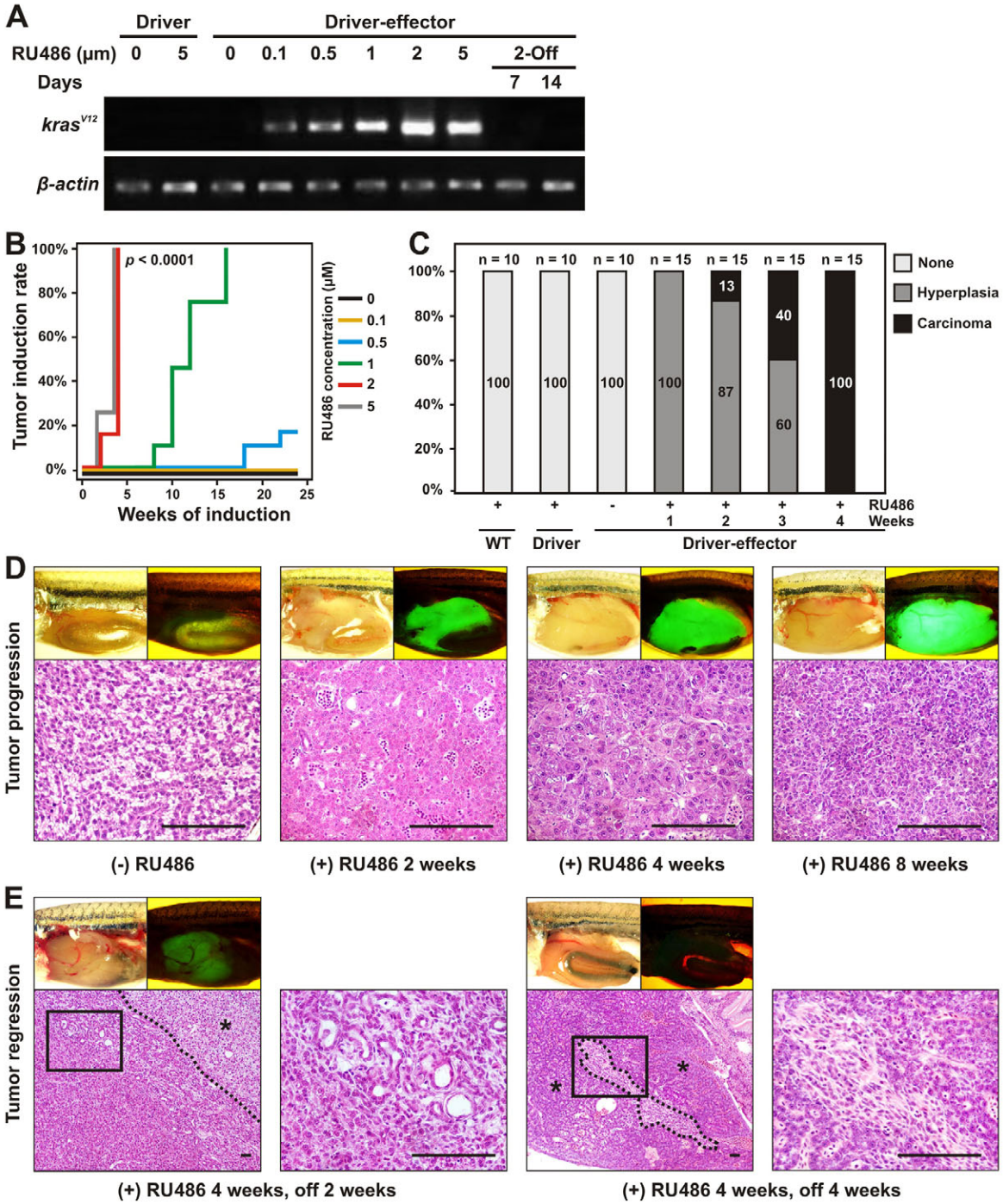

Fig. 2. Dosage-dependent induction of *kras*^{V12} expression and liver tumor induction and regression. (A) RT-PCR analysis of transgenic *kras*^{V12} transcripts in the liver of 1-month-old driver-effector double-transgenic larvae after 3 days of mifepristone (RU486) induction at different concentrations. Induced and non-induced driver transgenics together with non-induced driver-effectors were used as negative controls. β-actin was used as loading control. 2-Off, treatment with 2 mM mifepristone followed by withdrawal for 7 or 14 days. (B) Tumor induction rates for 1-month-old driver-effector fish under different concentrations of RU486 (*n*=20 in each group). (C) Statistics of tumor incidence as determined by histopathological analysis on induced driver-effector transgenics after 1-4 weeks of 2 μM RU486 treatment. WT, wild type. (D) Liver tumor progression in driver-effector fish induced by 2 μM mifepristone. The four panels represent different stages of liver tumorigenesis starting from normal control liver on the left to hyperplastic liver (HL) (2 weeks), HCC (4 weeks) and hepatoblastoma in mixed HCC (8 weeks). Each panel contains brightfield and fluorescent images of gross liver morphology (top) and a relevant histological image (bottom). (E) Liver tumor regression after mifepristone withdrawal. Following treatment of 2 μM RU486 for 4 weeks, driver-effector fish developed EGFP-labeled HCC and their exposure to RU486 was then terminated. Histological sections from two representative fish after RU486 removal for 2 and 4 weeks are shown. Dotted areas showed tumor shrinkage with marked peripheral scarring, whereas asterisks indicate surrounding normal hepatic tissue. (+) and (–) indicate RU486-treated and untreated fish, respectively. Boxed areas are shown enlarged on the right. Scale bars: 100 μm.

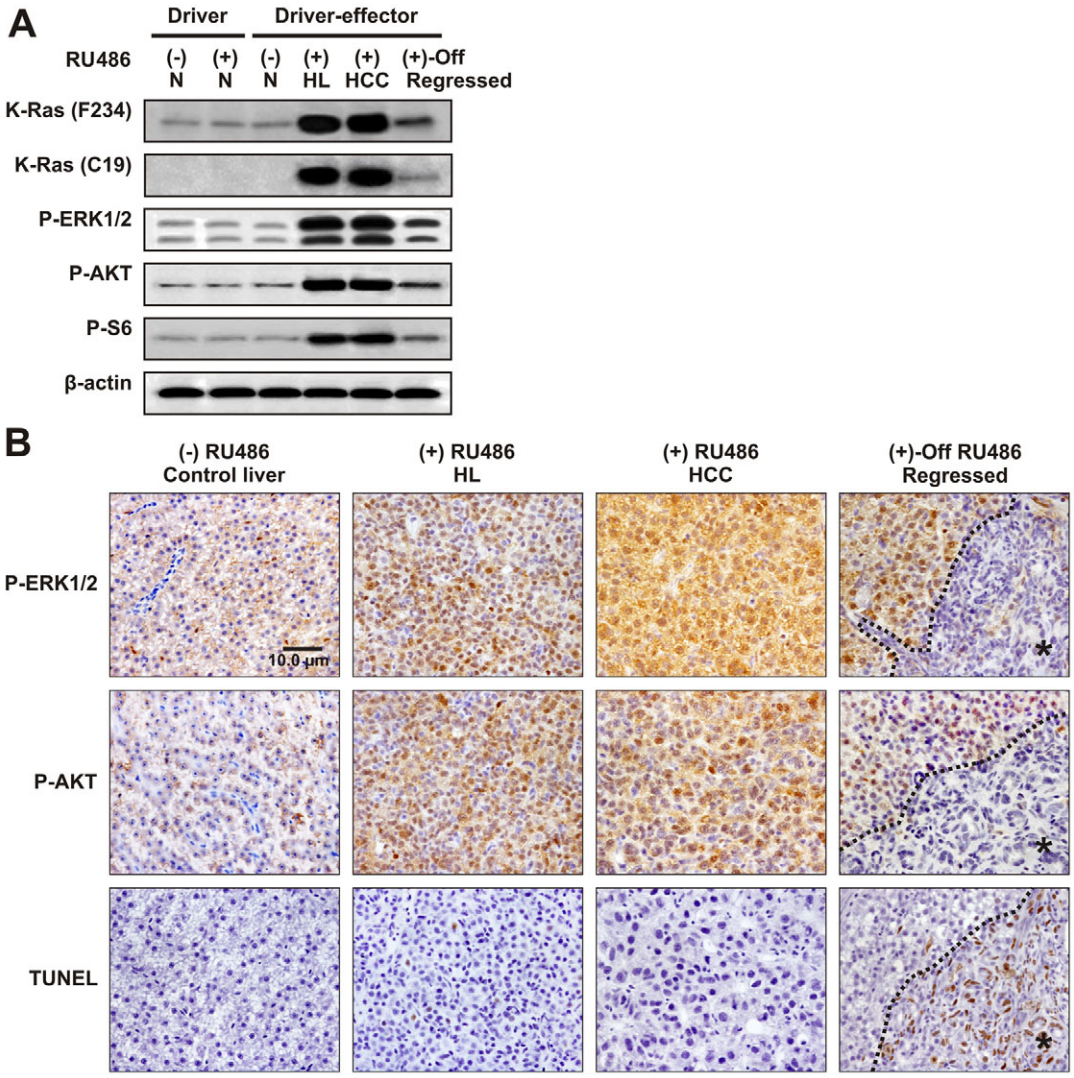

Fig. 3. Roles of the Raf-MEK-ERK and PI3K-AKT-mTOR pathways during *kras*^{V12} tumor progression and regression. (A) Western blots using total liver proteins from induced driver-effector fish with HL or HCC, as well as regressed liver samples, to detect total Kras (F234), mutant Kras-2B (C19) isoform, phospho-ERK1/2 (P-ERK1/2), P-AKT and P-S6 proteins. The non-induced driver, induced-driver and non-induced driver-effector having normal liver (N) served as controls. β-actin, internal control for equal loading. (B) Immunohistochemical staining showing phospho-ERK1/2 and -AKT protein as well as apoptotic cells (TUNEL) during *kras*^{V12}-dependent liver tumor progression and regression. Asterisks and dotted lines indicate the region of tumor scar.

also recovered the 'normal' liver phenotype in 57% or 69% of larvae, respectively. However, these results implied that inhibition of solely Raf-MEK-ERK or PI3K-AKT-mTOR pathways was insufficient to completely suppress the hyperplastic liver induced by *kras*^{V12}. Thus, co-treatment of PD98059 and LY294002 or rapamycin was performed to inhibit both pathways. Results revealed that blocking both pathways led to a more pronounced anti-tumorigenic effect (in 78-96% of larvae) (Fig. 4A,B). Western blotting using whole larvae lysates was also performed to confirm the outcomes of inhibitor treatments (Fig. 4C). Although all inhibitors significantly inhibited their targets, individually blocking either the Raf-MEK-ERK or PI3K-AKT-mTOR pathway did not affect activity of the other pathway, indicating the specificity of these inhibitors. The combination of both PD98059 and LY294002 showed a substantial decrease in phospho-ERK, phospho-AKT and phospho-S6 levels. However, only phospho-ERK and phospho-S6 levels were suppressed when PD98059 and rapamycin were used in co-treatment. Collectively, these results implied that both the Raf-MEK-ERK and PI3K-AKT-mTOR pathways need to be inhibited for suppression of tumorigenesis induced by Kras, as summarized in Fig. 4D.

DISCUSSION

Striking similarities between zebrafish and human tumors at the histological and molecular level has strengthened the rationale of using zebrafish as a laboratory cancer model over the past few years (Amatruda and Patton, 2008; Lam et al., 2006; Langenau et al., 2007; Nguyen et al., 2011). In addition, effective transgenic techniques have been successfully employed in zebrafish, allowing the use of zebrafish in modeling various human cancer types (Liu and Leach,

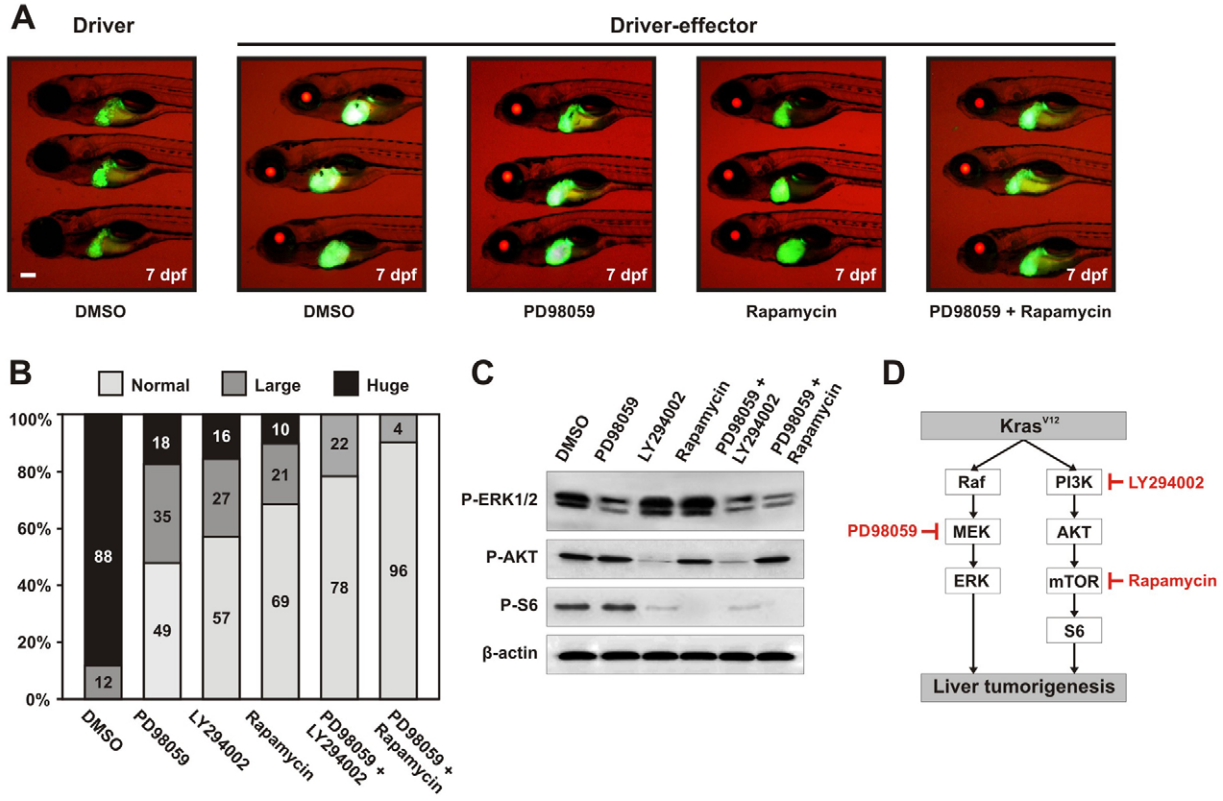

Fig. 4. Suppression of liver tumorigenesis by inhibition of the Raf-MEK-ERK and PI3K-AKT-mTOR pathways. (A) Fluorescent images showing representative mifepristone-induced *EGFP-kras*^{V12} driver-effector larvae at 7 dpf treated with different inhibitors, as compared with the DMSO-treated driver and driver-effector transgenics as controls. Scale bar: 200 µm. (B) Comparison of the anti-HL effect of inhibitors in transgenic larvae at 7 dpf. The liver size of treated larvae was classified as 'normal' if it was the same as the liver in driver transgenics, 'huge' if it remained enlarged/hyperplasia, or 'large' if it was larger than normal liver, but smaller than hyperplasia after 4 days of inhibitor treatment. (C) Lysates extracted from whole transgenic larvae treated with the indicated inhibitors were immunoblotted for phospho-ERK (P-ERK), P-AKT and P-S6. β-actin, internal control for equal loading. (D) Proposed inhibitor treatments to suppress Kras^{V12}-induced liver tumorigenesis via targeting both the Raf-MEK-ERK and PI3K-AKT-mTOR pathways.

2011). However, most of the transgenic systems have employed constitutive expression of an oncogene under control of a tissue-specific promoter to induce tumor growth, including *Myc*-induced leukemia, *BRAF*^{V600F}-induced melanoma, *KRAS*^{G12D}-induced rhabdomyosarcoma and pancreatic adenocarcinoma, and *kras*^{V12}-induced HCC (Langenau et al., 2003; Langenau et al., 2007; Nguyen et al., 2011; Park et al., 2008; Patton et al., 2005). Although this method offered a simple way to obtain stable transgenic zebrafish and a rapid test for oncogenicity of the transgenes in causing tumors, these models often developed severe cancers before the fish reached reproductive maturity, hindering maintenance of these transgenic lines (Langenau et al., 2003; Langenau et al., 2007; Nguyen et al., 2011). In addition, transgene expression at earlier stages of development caused severe embryonic defects that obscure the roles of the transgene at later stages (Nguyen et al., 2011). Therefore, improved techniques that permit switching gene expression on and off would help to overcome these problems.

In this study, using the mifepristone-inducible LexPR system (Emelyanov and Parinov, 2008), we have generated an important liver cancer model allowing for inducible and reversible control of *kras*^{V12} expression in the liver of transgenic zebrafish. The level of transgene expression was controlled by administering different concentrations of mifepristone, and a dosage-dependent *kras*^{V12} expression and induction of liver tumors was observed. Interestingly, 100% of transgenics that were treated with 2 µM mifepristone developed full-blown HCC after 1 month of treatment, demonstrating efficient tumor induction in this transgenic model. A schematic summary of our observations on tumor progression is presented in Fig. 5. Inducible *kras*^{V12} expression also permits temporal control of liver tumor onset to prevent early lethality, thereby allowing the propagation of stable transgenic models for long-term studies. These attributes enable us to overcome limitations that were present in our previous liver cancer model that constitutively expresses *kras*^{V12}, such as early oncogenic toxicity and/or lethality and low penetrance of tumor phenotype (Nguyen et al., 2011). Another interesting observation of this transgenic model is that full-blown HCC could be regressed to nearly normal liver upon Kras inactivation after mifepristone withdrawal; thus, these liver tumors seemed to be *kras*^{V12} addicted for their continuous growth and survival. Our data, together with numerous evidences that support the concept of 'oncogene addiction' derived from mouse models and human cancer cell lines, provided a rationale for molecular targeted therapies against Ras signaling (Engelman et al., 2008; Singh et al., 2009; Weinstein, 2002).

Recent therapeutic efforts on targeting mutant Ras have not been successful (Diaz-Flores and Shannon, 2007). Therefore,

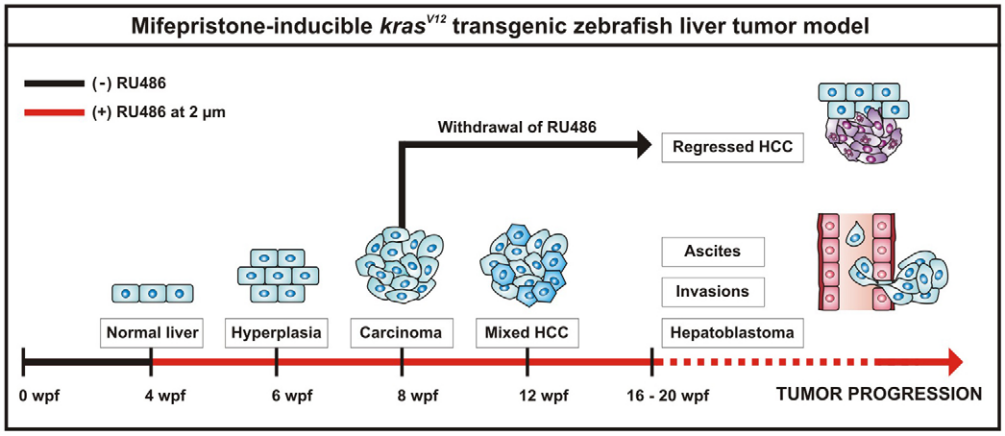

Fig. 5. Schematic summary of mifepristone-inducible *kras*^{V12} liver tumor model in transgenic zebrafish. Driver-effector fish can be induced for overexpression of *EGFP-kras*^{V12} with 2 µM mifepristone (RU486) from 4 weeks post-fertilization (wpf). Rapid and homogeneous liver tumorigenesis progresses from hyperplasia (6 wpf) to carcinoma (8 wpf) after 1 month of induction. Prolonged induction of transgenic fish (16-20 wpf) with mifepristone could lead to advanced liver cancer marked by the development of hepatoblastoma in mixed HCC, invasive HCCs and/or malignant ascites. By contrast, RU486 withdrawal results in tumor regression observed in transgenic fish with HCC (8 wpf). Purple cells represent scar tissue.

understanding the effector pathways that are engaged by oncogenic Ras is fundamental to inhibiting Ras-induced liver cancer. For this reason, we have addressed the importance of the two major pathways, Raf-MEK-ERK and PI3K-AKT-mTOR, as downstream Ras targets that are necessary for oncogenic Ras-driven signaling. Our finding emphasized that the Raf-MEK-ERK and PI3K-AKT-mTOR pathways were synergistically deregulated during liver tumor progression and regression in *kras*^{V12} transgenic fish. One of the advantages of this transgenic model is the feasibility of inducing *EGFP-kras*^{V12} expression in early-stage embryos to cause significantly enlarged livers that are easily visualized under fluorescent microscope. Thus, by using this advantage, we have tested several small chemical inhibitors that target different pathways for their effect on suppression of hyperplastic liver growth in the transgenic larvae. Our data clearly show that inhibition of a single pathway led to only modest suppression of hyperplastic liver growth. However, *kras*^{V12}-induced liver tumorigenesis is efficiently inhibited by blocking both pathways. This can be achieved by dual targeting of either MEK1/2 and PI3K or MEK1/2 and mTOR for inhibition of the two major Ras effector pathways. These results are consistent with previous reports that PI3K pathway activation renders *KRAS* mutant cancers insensitive to MEK inhibitors (Wee et al., 2009) or vice versa (Carracedo et al., 2008). Furthermore, our observations parallel clinical findings that blockade of the Raf-MEK-ERK and PI3K-AKT-mTOR pathways provide anti-tumoral effect in HCC and other Ras mutant tumors (Engelman et al., 2008; Newell et al., 2009). In this model, advanced liver cancer was marked by the development of mixed carcinoma, hepatoblastoma, malignant ascites or invasions of tumor cells into blood vessels or neighboring tissues (metastases) in transgenic fish. These symptoms are also found in severe stages of human liver cancers (Lambrecht et al., 2011; Roncalli et al., 2010; Yamazaki et al., 2004). The arising of advanced liver cancer in transgenic fish after long-term induction is potentially due to additional mutations that eventually cause an irreversible malignant phenotype. Thus, it would be interesting to use the current model in future studies to identify these mutations, which might shed new light on the molecular mechanisms that drive HCC and other types of liver tumor to which Ras has been linked. Recently, the development of hepatoblastoma has also been found in Noonan syndrome patients, who have constitutively activated Ras-ERK signaling (Yoshida et al., 2008). The PI3K-AKT pathway has also been found to play an essential role in growth and survival of hepatoblastoma cell lines (Hartmann et al., 2009). In line with these findings, activation of the two Ras downstream pathways, ERK and AKT, was observed in hepatoblastoma in our model (supplementary material Fig. S2), suggesting the ubiquitous role of Ras signaling in the initiation and development of a wide range of hepatocellular cancers.

By transcriptomic analyses, we have previously uncovered the overall molecular mechanisms and gene signatures underlying *kras*^{V12} liver tumorigenesis in two different stages, hyperplastic liver and HCC (Nguyen et al., 2011). Because it is possible to activate oncogenic *kras*^{V12} expression from any developmental stage and induce liver tumors synchronously, the current inducible *kras*^{V12} transgenic model provides an excellent opportunity to analyze the detailed molecular events in early liver tumor initiation and progression. On the basis of effectors engaged by Ras and significant utilities of the zebrafish system, we envisage the mifepristone-inducible *kras*^{V12} liver cancer model being useful for high-throughput screens of anti-cancer drugs. Owing to the rapid tumor onset in this model and the feasibility of performing large-scale mutagenesis, it is interesting to perform mutagenesis, such as by ethylnitrosourea (ENU) or by retroviral integration, to identify mutations that can delay or enhance tumor progression and even cause early metastasis. Alternatively, this can be achieved by overexpressing a second transgene in *kras*^{V12} transgenics. Because the oncogenicity of Ras is highly dependent on cellular context and intensity of Ras signaling (Guerra et al., 2003; Nguyen et al., 2011; Sarkisian et al., 2007), our mifepristone-inducible *kras*^{V12} transgenic zebrafish offers a potential model for further studies to assess these effects on Ras-induced liver tumorigenesis.

METHODS

Zebrafish maintenance

Zebrafish were maintained according to established protocols (Westerfield, 2000). All experiments involving animals were approved by the Institutional Animal Care and Use Committee (IACUC) of the National University of Singapore. Transgenic zebrafish generated from this study are available upon request.

Plasmid constructs and generation of transgenic fish using the *Ac/Ds* transposon system

The liver-driver construct was made by replacing *krt8* promoter of *pDs(krt8:LPR-LOP:G4)* (Emelyanov and Parinov, 2008) with the *fabp10* promoter at *Xho*I and *Asc*I sites (Fig. 1). The Kras effector construct was generated by inserting the amplified $kras^{V12}$ mutant digested with *Not*I and *Sac*II enzymes (Nguyen et al., 2011) into the *Xho*I and *Asc*I sites of the *pDs(cry:C-LOP:Ch)* vector (Emelyanov and Parinov, 2008). Synthesis of Ac transposase RNA and microinjection were performed as previously described (Emelyanov et al., 2006). Basically, 5-10 pg of plasmid DNA with 25-50 pg of in vitro synthesized transposase RNA was co-injected into zebrafish embryos at the one- to two-cell stage. The injected embryos were raised to adults and out-crossed to wild-type fish for testing germline transmission.

One-step RT-PCR

Liver RNAs were isolated using TriZOL (Invitrogen). A total of 1 µg RNA was used as a template to synthesize cDNA in a 20 µl RT-PCR reaction mixture containing 1 µl of one-step RT-PCR enzyme mix (Qiagen). Primers used in the one-step RT-PCR are as follows: $kras^{V12}$ forward, 5′-CGACCACTACCAGCAGAACA-3′ (targeting the *EGFP* region); $kras^{V12}$ reverse, 5′-GCTTTTGCCTACGCCTACAG-3′; Bactin-Forward, 5′-CCACCTTAAATGGCCTAGCA-3′; Bactin-Reverse, 5′-CATTGTGAGGAGGGCAAAGT-3′.

Tumor screening and histopathological analysis

Each group of induced driver-effector double-transgenic fish with different mifepristone concentrations was screened under the fluorescent Nikon SMZ1600 stereomicroscope every week to determine the rate of tumor induction. Liver tumor in induced double-transgenic fish was defined as EGFP-marked liver enlarged to at least twice the size of a normal liver in driver transgenics. All tumor-bearing fish were dissected to open the abdominal area and pictured by the Nikon DXM1200F digital camera. Fish were then fixed in Bouin's fixative, embedded in paraffin, sagittal sectioned, and stained with hematoxylin and eosin preceding histopathological diagnosis to confirm the liver lesion (Nguyen et al., 2011).

Immunoblotting and immunohistochemical analyses

Immunoblotting and immunohistochemical analyses were carried out as described previously (Nguyen et al., 2011). For western blotting, samples were lysed in the lysis buffer (10 mM Tris-HCl, pH 7.4, and 1% SDS) containing Complete Protease Inhibitor Cocktail (Roche). Proteins were resolved by SDS-PAGE and transferred to PVDF membrane. Non-specific sites were blocked with SuperBlock blocking buffer (Pierce Biotechnology) before incubation with secondary antibodies. Signals were detected using chemiluminescence (Pierce Biotechnology) and exposure to X-ray film (Kodak). For immunohistochemistry, 5-µm formalin-fixed and paraffin-embedded tissue sections were first boiled for antigen retrieval in 10 mM citrate buffer, pH 6.0 or 9.0, treated with 3% hydrogen peroxide and blocked using the SuperBlock blocking buffer (Pierce Biotechnology). After incubation with primary antibody overnight at 4°C and with secondary antibody for 1 hour at 28°C, signals were detected using the Metal Enhanced DAB Substrate Kit (Pierce Biotechnology). Sections were then counterstained with hematoxylin, dehydrated and permanently mounted. Primary antibodies used in this study included anti-Kras (F234) for detecting ubiquitously expressed Kras (Santa Cruz Biotechnology), anti-Kras-2B (C19) for the C-terminus of the Kras-2B splice variant (Santa Cruz Biotechnology), phospho-ERK1/2 (Thr202/Tyr204; Cell Signaling Technology), phospho-AKT (Ser473; Cell Signaling Technology), phospho-S6 (Ser235/236; Cell Signaling Technology) and β-actin (Sigma). Anti-mouse or anti-rabbit secondary antibodies were purchased from Cell Signaling Technology.

TUNEL staining

The single- and double-stranded DNA breaks that occur at the early stages in apoptotic cells in liver tissues were stained using the in situ Cell Death Detection Kit according to the manufacturer's protocol (Roche). Cryostat sections were prepared, fixed and permeabilized as described previously (Nguyen et al., 2011). Subsequently, sections were incubated with the TUNEL reaction mixture that contains TdT and fluorescein-dUTP conjugated with peroxidase. After washing, converter-POD was added and signal was developed using the Metal Enhanced DAB Substrate Kit (Pierce Biotechnology). Finally, sections were counterstained with hematoxylin prior to microscope analysis.

Inhibitor treatment

Driver-effector double-transgenic larvae were arrayed in a 96-well plate at a density of two larvae per well, to which 200 µl E3 embryo medium was added (Westerfield, 2000), which contained 1 µM mifepristone (Sigma) and one or two of the following chemical inhibitors: 10 µM PD98059 (Calbiochem), 10 µM U0126 (Sigma), 10 µM LY294002 (Sigma), 0.7 µM rapamycin (Calbiochem), 10 µM PD98059 + 10 µM LY294002, or 10 µM PD98059 + 0.7 µM rapamycin. Each treatment group included 100 larvae and experiments were repeated at least twice independently. Suitable concentrations of inhibitors were determined based on preliminary experiments for developmental toxicity (A.E. and S.P., unpublished data). The treatments were initiated from 3 dpf and continued until 7 dpf, except that treatments with rapamycin were started at 3.5 dpf to avoid its adverse effects on normal development (Makky et al., 2007). In parallel, the double-transgenic and driver-alone larvae were incubated with 1 µM mifepristone and 0.01% DMSO, respectively, as controls. All groups were incubated in the dark at 28°C.

Statistical analysis

The log-rank Kaplan-Meier analysis was used to compare rates of tumor induction between groups of induced transgenic fish. A $P<0.01$ was chosen to be statistically significant.

FUNDING

This work was supported by the Biomedical Research Council of Singapore [grant number 07/1/21/19/499].

TRANSLATIONAL IMPACT

Clinical issue

The Ras proto-oncogene is a central player in intracellular signal transduction pathways and is one of the most frequently mutated oncogenes in many human cancers. Activation of Ras signaling is a pervasive and characteristic feature of hepatocellular carcinoma (HCC), one of the most lethal cancers worldwide. Recently, pharmacological inhibition of Ras signaling has shown promising anti-tumoral activity in HCC patients, providing a rationale to identify more drug targets in the Ras signaling pathway and downstream effector pathways. The relatively low cost and potential to develop high-throughput screening platforms with zebrafish means that developing a Ras-mediated model of HCC in this model organism is a promising strategy to understand the molecular mechanisms of liver tumor initiation and progression, and to identify potential therapeutic targets in HCC.

Results

In this study, the authors generate a transgenic zebrafish model in which liver-specific expression of *EGFP-kras*^{V12} is induced only by the administration of the steroid compound mifepristone. Rapid progression of liver tumors is observed following mifepristone administration: within 1 month, HCC occurs in 100% of fish that receive the compound. These liver tumors rapidly regress on removal of mifepristone, indicating that continued *kras*^{V12} expression is required for tumor maintenance. Molecular analyses indicate that both the Raf-MEK-ERK and PI3K-AKT-mTOR signaling pathways are activated during *kras*^{V12}-mediated liver tumorigenesis. By testing the effect of specific inhibitors on rapidly growing hyperplastic livers in mifepristone-induced transgenic larvae, the authors assess the roles of these two signaling pathways in tumor suppression. These experiments show that inhibition of either the Raf-MEK-ERK or the PI3K-AKT-mTOR signaling pathway suppresses the overgrowth of hyperplastic livers, and that combined inhibition of both pathways has a more potent suppressive effect.

Implications and future directions

This group previously developed a zebrafish transgenic model of HCC constitutively expressing *kras*^{V12} that recapitulates the molecular hallmarks of human HCC, but with low incidence and late onset. The ability to specifically and inducibly express *kras*^{V12} in the new transgenic model reported here provides a better system to capture the molecular events of liver tumor initiation and progression. This inducible zebrafish HCC model can be developed for high-throughput chemical screening for novel cancer targets and/or inhibitors of Ras-mediated tumorigenesis. Furthermore, genome-wide mutagenesis could be performed to identify genes that promote or suppress liver tumorigenesis.

COMPETING INTERESTS

The authors declare that they do not have any competing or financial interests.

AUTHOR CONTRIBUTIONS

A.T.N., A.E., S.P. and Z.G. conceived and designed the study. A.T.N. and C.H.V.K. performed the experiments. A.T.N., A.E., C.H.V.K., J.M.S., S.P. and Z.G. analyzed and interpreted the data. A.E. and J.M.S. supported techniques. A.T.N., C.H.V.K. and Z.G. wrote the manuscript. A.E., S.P. and Z.G. supervised the study.

SUPPLEMENTARY MATERIAL

Supplementary material for this article is available at
http://dmm.biologists.org/lookup/suppl/doi:10.1242/dmm.008367/-/DC1

REFERENCES

Amatruda, J. F. and Patton, E. E. (2008). Genetic models of cancer in zebrafish. *Int. Rev. Cell Mol. Biol.* **271**, 1-34.

Calvisi, D. F., Ladu, S., Gorden, A., Farina, M., Conner, E. A., Lee, J. S., Factor, V. M. and Thorgeirsson, S. S. (2006). Ubiquitous activation of Ras and Jak/Stat pathways in human HCC. *Gastroenterology* **130**, 1117-1128.

Carracedo, A., Ma, L., Teruya-Feldstein, J., Rojo, F., Salmena, L., Alimonti, A., Egia, A., Sasaki, A. T., Thomas, G., Kozma, S. C. et al. (2008). Inhibition of mTORC1 leads to MAPK pathway activation through a PI3K-dependent feedback loop in human cancer. *J. Clin. Invest.* **118**, 3065-3074.

Diaz-Flores, E. and Shannon, K. (2007). Targeting oncogenic Ras. *Genes Dev.* **21**, 1989-1992.

Downward, J. (2003). Targeting RAS signalling pathways in cancer therapy. *Nat. Rev. Cancer* **3**, 11-22.

Emelyanov, A. and Parinov, S. (2008). Mifepristone-inducible LexPR system to drive and control gene expression in transgenic zebrafish. *Dev. Biol.* **320**, 113-121.

Emelyanov, A., Gao, Y., Naqvi, N. I. and Parinov, S. (2006). Trans-kingdom transposition of the maize dissociation element. *Genetics* **174**, 1095-1104.

Engelman, J. A., Chen, L., Tan, X., Crosby, K., Guimaraes, A. R., Upadhyay, R., Maira, M., McNamara, K., Perera, S. A., Song, Y. et al. (2008). Effective use of PI3K and MEK inhibitors to treat mutant Kras G12D and PIK3CA H1047R murine lung cancers. *Nat. Med.* **14**, 1351-1356.

Farazi, P. A. and DePinho, R. A. (2006). Hepatocellular carcinoma pathogenesis: from genes to environment. *Nat. Rev. Cancer* **6**, 674-687.

Gomaa, A. I., Khan, S. A., Toledano, M. B., Waked, I. and Taylor-Robinson, S. D. (2008). Hepatocellular carcinoma: epidemiology, risk factors and pathogenesis. *World J. Gastroenterol.* **14**, 4300-4308.

Guerra, C., Mijimolle, N., Dhawahir, A., Dubus, P., Barradas, M., Serrano, M., Campuzano, V. and Barbacid, M. (2003). Tumor induction by an endogenous K-ras oncogene is highly dependent on cellular context. *Cancer Cell* **4**, 111-120.

Hartmann, W., Küchler, J., Koch, A., Friedrichs, N., Waha, A., Endl, E., Czerwitzki, J., Metzger, D., Steiner, S., Wurst, P. et al. (2009). Activation of phosphatidylinositol-3′-kinase/AKT signaling is essential in hepatoblastoma survival. *Clin. Cancer Res.* **15**, 4538-4545.

Her, G. M., Chiang, C. C., Chen, W. Y. and Wu, J. L. (2003). In vivo studies of liver-type fatty acid binding protein (L-FABP) gene expression in liver of transgenic zebrafish (*Danio rerio*). *FEBS Lett.* **538**, 125-133.

Korzh, S., Pan, X., Garcia-Lecea, M., Winata, C. L., Pan, X., Wohland, T., Korzh, V. and Gong, Z. (2008). Requirement of vasculogenesis and blood circulation in late stages of liver growth in zebrafish. *BMC Dev. Biol.* **8**, 84.

Lam, S. H., Wu, Y. L., Vega, V. B., Miller, L. D., Spitsbergen, J., Tong, Y., Zhan, H., Govindarajan, K. R., Lee, S., Mathavan, S. et al. (2006). Conservation of gene expression signatures between zebrafish and human liver tumors and tumor progression. *Nat. Biotechnol.* **24**, 73-75.

Lambrecht, R. W., Sterling, R. K., Naishadham, D., Stoddard, A. M., Rogers, T., Morishima, C., Morgan, T. R., Bonkovsky, H. L. and HALT-C Trial Group (2011). Iron levels in hepatocytes and portal tract cells predict progression and outcomes of patients with advanced chronic hepatitis C. *Gastroenterology* **140**, 1490-1500.

Langenau, D. M., Traver, D., Ferrando, A. A., Kutok, J. L., Aster, J. C., Kanki, J. P., Lin, S., Prochownik, E., Trede, N. S., Zon, L. I. et al. (2003). Myc-induced T cell leukemia in transgenic zebrafish. *Science* **299**, 887-890.

Langenau, D. M., Keefe, M. D., Storer, N. Y., Guyon, J. R., Kutok, J. L., Le, X., Goessling, W., Neuberg, D. S., Kunkel, L. M. and Zon, L. I. (2007). Effects of RAS on the genesis of embryonal rhabdomyosarcoma. *Genes Dev.* **21**, 1382-1395.

Liu, S. and Leach, S. D. (2011). Zebrafish models for cancer. *Annu. Rev. Pathol.* **6**, 71-93.

Llovet, J. M. and Bruix, J. (2008). Molecular targeted therapies in hepatocellular carcinoma. *Hepatology* **48**, 1312-1327.

Makky, K., Tekiela, J. and Mayer, A. N. (2007). Target of rapamycin (TOR) signaling controls epithelial morphogenesis in the vertebrate intestine. *Dev. Biol.* **303**, 501-513.

Newell, P., Toffanin, S., Villanueva, A., Chiang, D. Y., Minguez, B., Cabellos, L., Savic, R., Hoshida, Y., Lim, K. H., Melgar-Lesmes, P. et al. (2009). Ras pathway activation in hepatocellular carcinoma and anti-tumoral effect of combined sorafenib and rapamycin in vivo. *J. Hepatol.* **51**, 725-733.

Nguyen, A. T., Emelyanov, A., Koh, C. H. V., Spitsbergen, J. M., Lam, S. H., Mathavan, S., Parinov, S. and Gong, Z. (2011). A high level of liver-specific expression of oncogenic Kras^{V12} drives robust liver tumorigenesis in transgenic zebrafish. *Dis. Model. Mech.* **4** (Epub ahead of print).

Park, S. W., Davison, J. M., Rhee, J., Hruban, R. H., Maitra, A. and Leach, S. D. (2008). Oncogenic KRAS induces progenitor cell expansion and malignant transformation in zebrafish exocrine pancreas. *Gastroenterology* **134**, 2080-2090.

Patton, E. E., Widlund, H. R., Kutok, J. L., Kopani, K. R., Amatruda, J. F., Murphey, R. D., Berghmans, S., Mayhall, E. A., Traver, D., Fletcher, C. D. et al. (2005). BRAF mutations are sufficient to promote nevi formation and cooperate with p53 in the genesis of melanoma. *Curr. Biol.* **15**, 249-254.

Roncalli, M., Park, Y. N. and DiTommaso, L. (2010). Histopathological classification of hepatocellular carcinoma. *Dig. Liver Dis.* **42**, S228-S234.

Sarkisian, C. J., Keister, B. A., Stairs, D. B., Boxer, R. B., Moody, S. E. and Chodosh, L. A. (2007). Dose-dependent oncogene-induced senescence in vivo and its evasion during mammary tumorigenesis. *Nat. Cell Biol.* **9**, 493-505.

Schmidt, C. M., McKillop, I. H., Cahill, P. A. and Sitzmann, J. V. (1997). Increased MAPK expression and activity in primary human hepatocellular carcinoma. *Biochem. Biophys. Res. Commun.* **236**, 54-58.

Singh, A., Greninger, P., Rhodes, D., Koopman, L., Violette, S., Bardeesy, N. and Settleman, J. (2009). A gene expression signature associated with "K-Ras addiction" reveals regulators of EMT and tumor cell survival. *Cancer Cell* **15**, 489-500.

Villanueva, A. and Llovet, J. M. (2011). Targeted therapies for hepatocellular carcinoma. *Gastroenterology* **140**, 1410-1426.

Wee, S., Jagani, Z., Xiang, K. X., Loo, A., Dorsch, M., Yao, Y. M., Sellers, W. R., Lengauer, C. and Stegmeier, F. (2009). PI3K pathway activation mediates resistance to MEK inhibitors in KRAS mutant cancers. *Cancer Res.* **69**, 4286-4293.

Weinstein, I. B. (2002). Addiction to oncogenes-the Achilles heal of cancer. *Science* **297**, 63-64.

Westerfield, M. (2000). *The Zebrafish Book: A Guide for the Laboratory Use of Zebrafish (Danio rerio)*, 4th edn. Eugene, OR: University of Oregon Press.

Yamazaki, M., Ryu, M., Okazumi, S., Kondo, F., Cho, A., Okada, T., Takayama, W., Kawashima, T., Furuki, A. and Hirata, T. (2004). Hepatoblastoma in an adult A case report and clinical review of literatures. *Hepatol. Res.* **30**, 182-188.

Yoshida, R., Ogata, T., Masawa, N. and Nagai, T. (2008). Hepatoblastoma in a Noonan syndrome patient with a PTPN11 mutation. *Pediatr. Blood Cancer* **50**, 1274-1276.

Zender, L., Spector, M. S., Xue, W., Flemming, P., Cordon-Cardo, C., Silke, J., Fan, S. T., Luk, J. M., Wigler, M., Hannon, G. J. et al. (2006). Identification and validation of oncogenes in liver cancer using an integrative oncogenomic approach. *Cell* **125**, 1253-1267.

Zon, L. I. and Peterson, R. T. (2005). In vivo drug discovery in the zebrafish. *Nat. Rev. Drug Discov.* **4**, 35-44.